Cosmological Collider Signatures from Right-Handed Neutrino Loop

Chengcheng Han
Sun Yat-sen University

2026 Workshop on New Physics and Interdisciplinary Sciences (NPhiS 2026)
Nanjing Normal University

2026.5.16

Neutrino masses point to physics at very high scales

Why right-handed neutrinos?

- Neutrino oscillations imply nonzero neutrino masses.
- The seesaw mechanism gives a natural explanation for their small masses.
- It is also closely connected to leptogenesis and the baryon asymmetry.

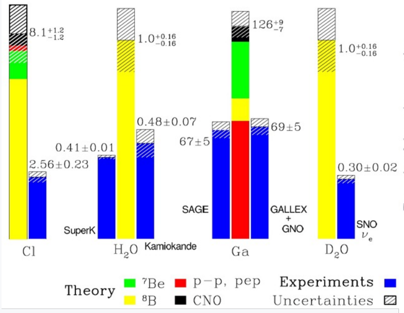

Solar Neutrino oscillations

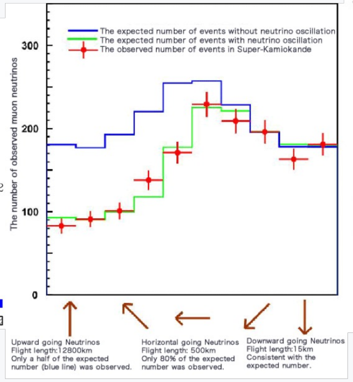

Atmospheric Neutrino Oscillations

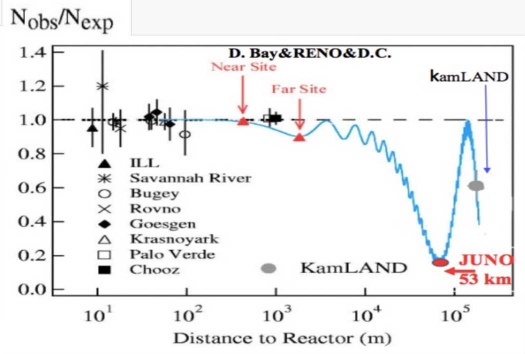

Reactor Neutrino Oscillations

If Yukawa couplings are O(1), the seesaw scale is typically $M_R \sim 10^{13\text{-}14}$ GeV, far beyond laboratory reach

Inflation

- Solving the initial condition problems: flatness problem, horizon problem
- Seeding the primordial anisotropies in CMB

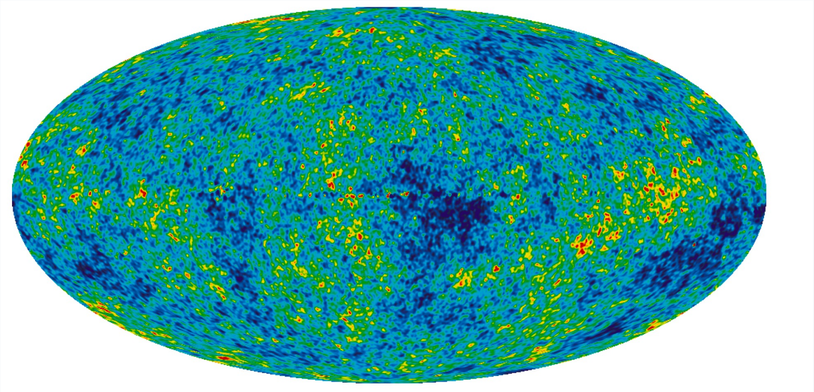

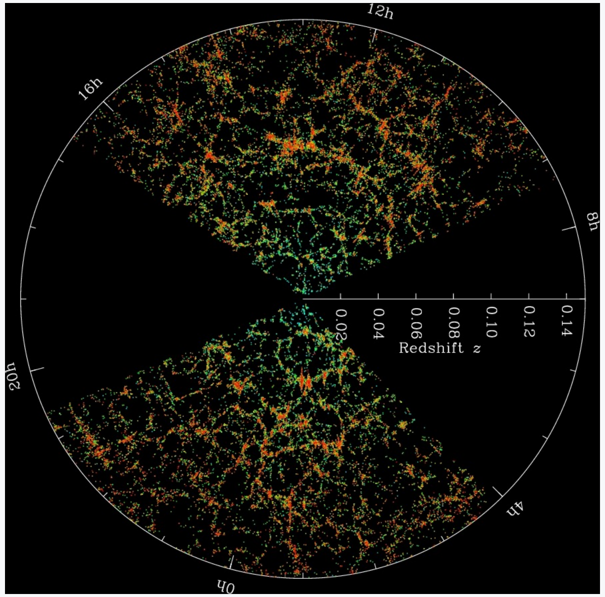

These tiny primordial fluctuations later grow into the large-scale structure of our universe.

Inflation and new physics

- During inflation, Hubble parameter is nearly constant(de Sitter universe), as high as ~10^{14} GeV
- In single-field inflation, the fluctuations are expected to be nearly Gaussian and approximately scale invariant.
- Non-Gaussianity is therefore a sensitive probe of additional fields coupled to the inflaton.

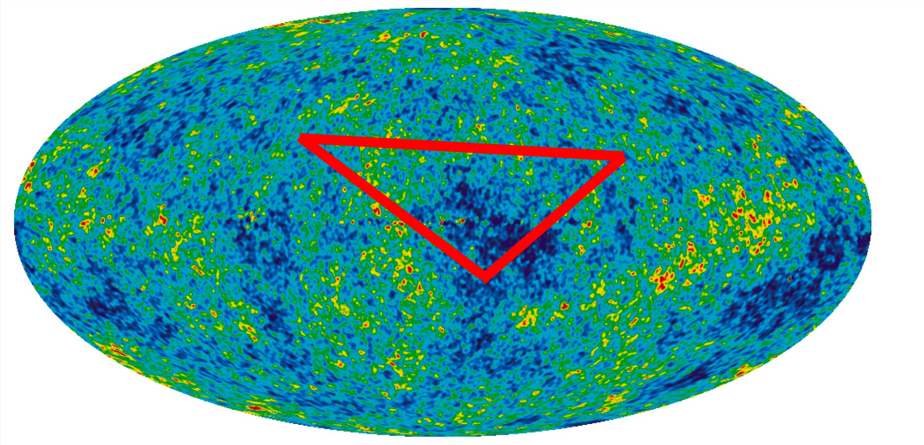

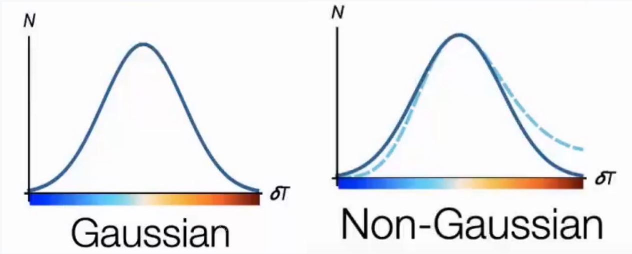

Current limit from Planck on local type f_{NL}~ O(10), future CMB observations, CMB S4, large scale structure observations DESI O(1), 21 cm tomography O(0.01-0.1)

Cosmological collider physics

X. Chen and Y. Wang, JCAP 04 (2010)027
N. Arkani-Hamed and J. Maldacena, arXiv:1503.08043

- Inflation can act as a high-energy collider sensitive to particles with mass ~ H
- Their mass and spin are encoded in non-analytic features of the squeezed bispectrum
- Particles with $m \sim H$ can produce oscillatory signals, whereas heavier states are increasingly suppressed

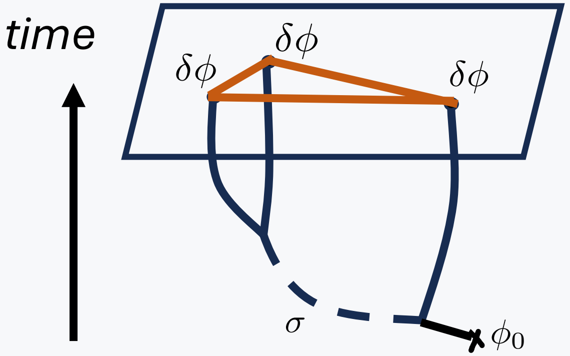

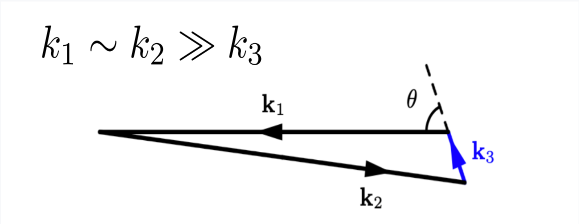

$$\tilde{\nu} = \sqrt{\frac{m^2}{H^2} - \frac{9}{4}}$$

$$\langle \delta\phi_{\mathbf{k_1}} \delta\phi_{\mathbf{k_2}} \delta\phi_{\mathbf{k_3}} \rangle \sim e^{-\pi\tilde{\nu}} \cos(\tilde{\nu} \log \frac{k_3}{k_1} + \delta) P_s(\cos\theta)$$

P. Daniel Meerburg, M. Münchmeyer, J. B. Muñoz, X. Chen, JCAP 03 (2017) 050

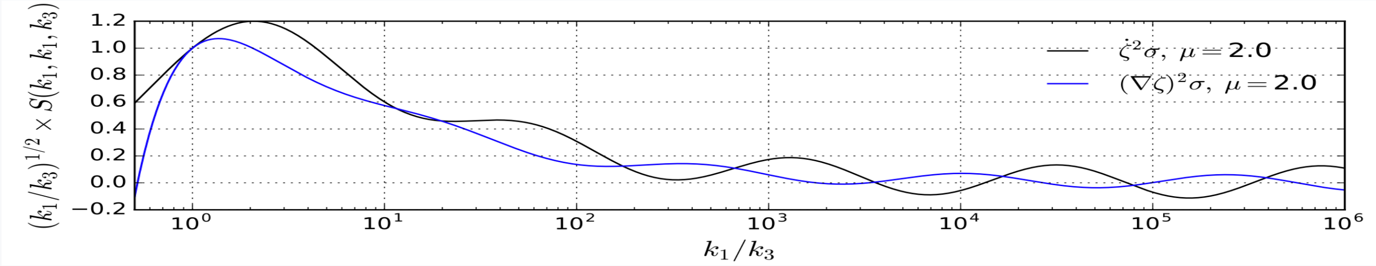

$$\langle \zeta^3 \rangle \equiv (2\pi)^3 \delta_D(\mathbf{k}_{123}) \frac{A^2}{(k_1 k_2 k_3)^2} S(k_1, k_2, k_3)$$

$$P_\zeta(k) = A/k^3$$

Where does the cosmological collider signal come from?

Consider a three-point correlation function mediated by a massive scalar field(m > 3/2 H)

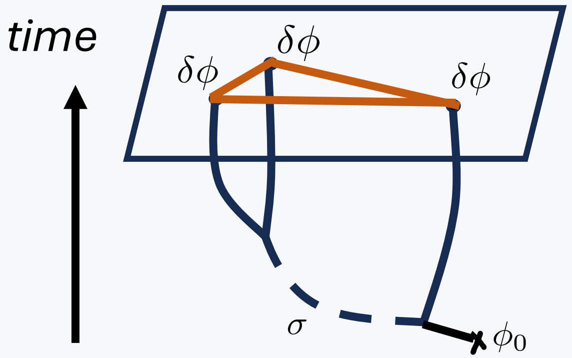

$$\ddot{\sigma}_{\mathbf{k}} + 3H\dot{\sigma}_{\mathbf{k}} + \frac{k^2}{a^2}\sigma_{\mathbf{k}} + m^2\sigma_{\mathbf{k}} = 0$$

$$\sigma_{\mathbf{k}}(\tau) = \frac{\sqrt{\pi}\,H}{2} e^{-\pi\tilde{\nu}/2}(-\tau)^{3/2}\mathrm{H}^{(1)}_{\mathrm{i}\tilde{\nu}}(-k\tau) \qquad \tilde{\nu} = \sqrt{\frac{m^2}{H^2} - \frac{9}{4}}$$

There are four Schwinger-Keldysh propagators

$$\begin{aligned}
D_{\oplus\oplus}(\mathbf{k};\tau_1,\tau_2) &= \sigma_{\mathbf{k}}(\tau_1)\sigma^*_{\mathbf{k}}(\tau_2)\,\theta(\tau_1-\tau_2) + \sigma^*_{\mathbf{k}}(\tau_1)\sigma_{\mathbf{k}}(\tau_2)\,\theta(\tau_2-\tau_1)\\
D_{\ominus\oplus}(\mathbf{k};\tau_1,\tau_2) &= \sigma^*_{\mathbf{k}}(\tau_1)\sigma_{\mathbf{k}}(\tau_2),\\
D_{\oplus\ominus}(\mathbf{k};\tau_1,\tau_2) &= \sigma_{\mathbf{k}}(\tau_1)\sigma^*_{\mathbf{k}}(\tau_2),\\
D_{\ominus\ominus}(\mathbf{k};\tau_1,\tau_2) &= \sigma^*_{\mathbf{k}}(\tau_1)\sigma_{\mathbf{k}}(\tau_2)\,\theta(\tau_1-\tau_2) + \sigma_{\mathbf{k}}(\tau_1)\sigma^*_{\mathbf{k}}(\tau_2)\,\theta(\tau_2-\tau_1)
\end{aligned}$$

These propagators contain non-analytic momentum dependence, in the late-time limit tau->0

$$[D_{\oplus\ominus}(\mathbf{k},\tau_1,\tau_2)]_{(\mathrm{NLoc})} = \frac{H^2(\tau_1\tau_2)^{3/2}}{4\pi}\left[\Gamma(-\mathrm{i}\tilde{\nu})^2\left(\frac{k^2\tau_1\tau_2}{4}\right)^{\mathrm{i}\tilde{\nu}} + \Gamma(\mathrm{i}\tilde{\nu})^2\left(\frac{k^2\tau_1\tau_2}{4}\right)^{-\mathrm{i}\tilde{\nu}}\right]$$

Massive particles generally induce cosmological collider signal

Key Questions for Right-Handed-Neutrino Cosmological Collider Signals

- Can right-handed neutrinos generate a cosmological-collider signal?
- How to compute it in a controlled way?
- Can the final signal be large enough to be observable?
- What is its angular structure?

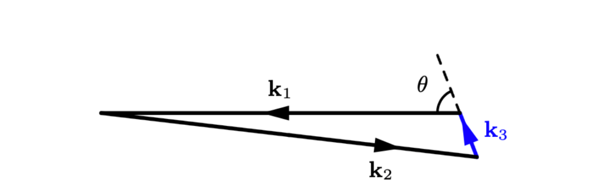

Model setup

We consider a shift-symmetric interaction between the inflaton background and RH neutrinos

$$\frac{1}{\Lambda}\,\partial_\mu\phi\,N^\dagger\bar{\sigma}^\mu N$$

- Perturbative control requires the cutoff scale $\Lambda > 60\,H$
- The same coupling induces an effective chemical potential for N $\quad \lambda \sim \dot{\phi}/\Lambda \qquad \dot{\phi} \simeq (60H)^2$
- The chemical potential could help to alleviate the suppression factor in cosmological signal

$$e^{-\pi m/H} \to e^{-\pi m^2/\lambda H}$$

Cosmological collider signals from fermions

Although substantial progress has been made in cosmological-collider signals in recent years, most studies have focused on scalar mediators, while fermionic signals remain much less explored due to their technical complexity.

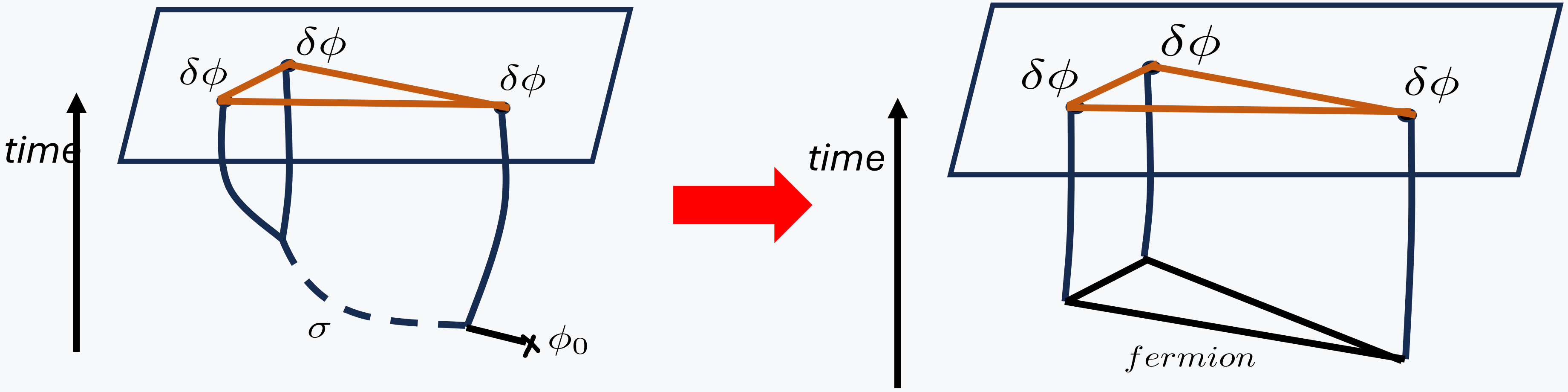

- For fermions, the leading cosmological-collider signal typically starts at loop level
- The mode functions are nontrivial in de Sitter space
- The loop-momentum integration must be handled carefully to isolate the nonlocal piece

Fermions in an inflationary background

$$\tilde{N}_\alpha(\tau,x)=\int\frac{d^3\mathbf{k}}{(2\pi)^3}\sum_{s=\pm}\left[\xi_{s,\alpha}(\tau,\mathbf{k})b_s(\mathbf{k})e^{\mathrm{i}\mathbf{k}\cdot\mathbf{x}}+\chi_{s,\alpha}(\tau,\mathbf{k})b_s^\dagger(\mathbf{k})e^{-\mathrm{i}\mathbf{k}\cdot\mathbf{x}}\right]$$

$$\tilde{M}_R=\frac{M_R}{H},\qquad \tilde{\lambda}=\frac{\lambda}{H},\qquad \lambda=\frac{\dot{\phi}_0}{\Lambda},\qquad \tilde{\nu}=\sqrt{\tilde{M}_R^2+\tilde{\lambda}^2}$$

$$\xi_{s,\alpha}(\tau,\mathbf{k})=u_s(\tau,\mathbf{k})\,h_{s,\alpha}(\mathbf{k}),\qquad \chi_s^{\dagger\dot{\alpha}}(\tau,\mathbf{k})=v_s(\tau,\mathbf{k})\,s\,h_{-s}^{\dagger\dot{\alpha}}(\mathbf{k}).$$

$$u_+(\tau,\mathbf{k})=\tilde{m}\frac{e^{+\pi\tilde{\lambda}/2}}{\sqrt{-2k\tau}}W_{-\frac{1}{2}-\mathrm{i}\tilde{\lambda},\mathrm{i}\tilde{\nu}}(2\mathrm{i}k\tau),\qquad v_+(\tau,\mathbf{k})=\frac{e^{+\pi\tilde{\lambda}/2}}{\sqrt{-2k\tau}}W_{\frac{1}{2}-\mathrm{i}\tilde{\lambda},\mathrm{i}\tilde{\nu}}(2\mathrm{i}k\tau),$$

$$u_-(\tau,\mathbf{k})=\frac{e^{-\pi\tilde{\lambda}/2}}{\sqrt{-2k\tau}}W_{\frac{1}{2}+\mathrm{i}\tilde{\lambda},\mathrm{i}\tilde{\nu}}(2\mathrm{i}k\tau),\qquad v_-(\tau,\mathbf{k})=\tilde{m}\frac{e^{-\pi\tilde{\lambda}/2}}{\sqrt{-2k\tau}}W_{-\frac{1}{2}+\mathrm{i}\tilde{\lambda},\mathrm{i}\tilde{\nu}}(2\mathrm{i}k\tau),$$

Two kinds of propagators appear, analogous to Weyl-fermion propagators in flat spacetime

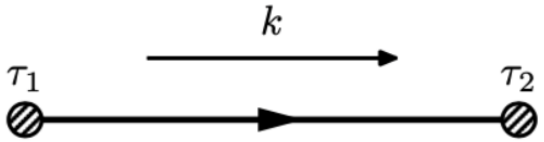

$$\equiv D_{ab\,\alpha\dot{\beta}}(\mathbf{k},\tau_1,\tau_2)$$

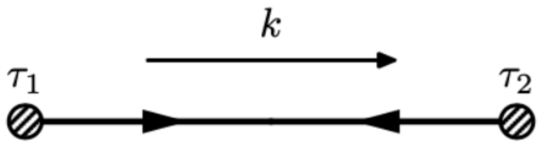

$$\equiv \hat{D}_{ab\alpha\beta}(\mathbf{k},\tau_1,\tau_2)$$

Eight inequivalent loop contractions (64 contributions after Schwinger-Keldysh index assignments)

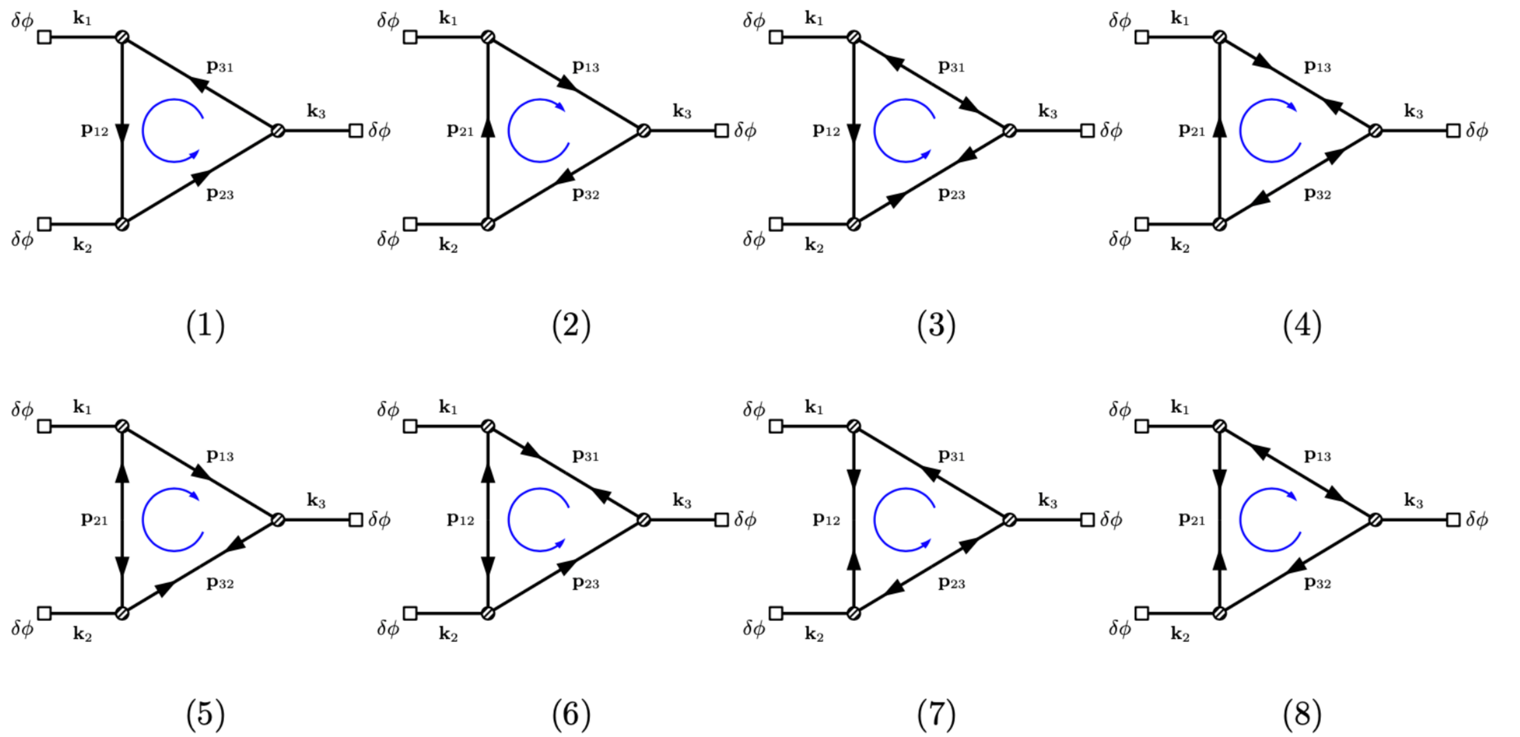

$$\langle\delta\phi(\mathbf{k}_1)\delta\phi(\mathbf{k}_2)\delta\phi(\mathbf{k}_3)\rangle' = \sum_{j=1}^{8}\langle\delta\phi(\mathbf{k}_1)\delta\phi(\mathbf{k}_2)\delta\phi(\mathbf{k}_3)\rangle'^{(j)}$$

$$= \sum_{a,b,c=\pm} abc\left(\frac{-\mathrm{i}}{\Lambda}\right)^3\int_{-\infty}^{0^-}\mathrm{d}\tau_1\mathrm{d}\tau_2\mathrm{d}\tau_3\,\mathcal{F}_{\mu a}(\mathbf{k}_1,\tau_1)\mathcal{F}_{\nu b}(\mathbf{k}_2,\tau_2)\mathcal{F}_{\lambda c}(\mathbf{k}_3,\tau_3)\int\frac{\mathrm{d}^3\mathbf{q}}{(2\pi)^3}\sum_{j=1}^{8}\mathcal{Y}^{\mu\nu\lambda}_{abc}(j)$$

$$\mathcal{F}_{\mu a}(\mathbf{k},\tau) = \begin{pmatrix}\partial_\tau G_a(k;\tau)\\ \mathrm{i}\mathbf{k}G_a(k;\tau)\end{pmatrix} = \frac{H^2}{2k^3}\begin{pmatrix}k^2\tau\\ \mathrm{i}\mathbf{k}(1-\mathrm{i}ak\tau)\end{pmatrix}e^{+\mathrm{i}ak\tau}$$

In the relevant soft limit, the loop diagram factorizes and the nonlocal signal can be isolated

Z. Qin, Z.Z. Xianyu, JHEP 09 (2023) 116

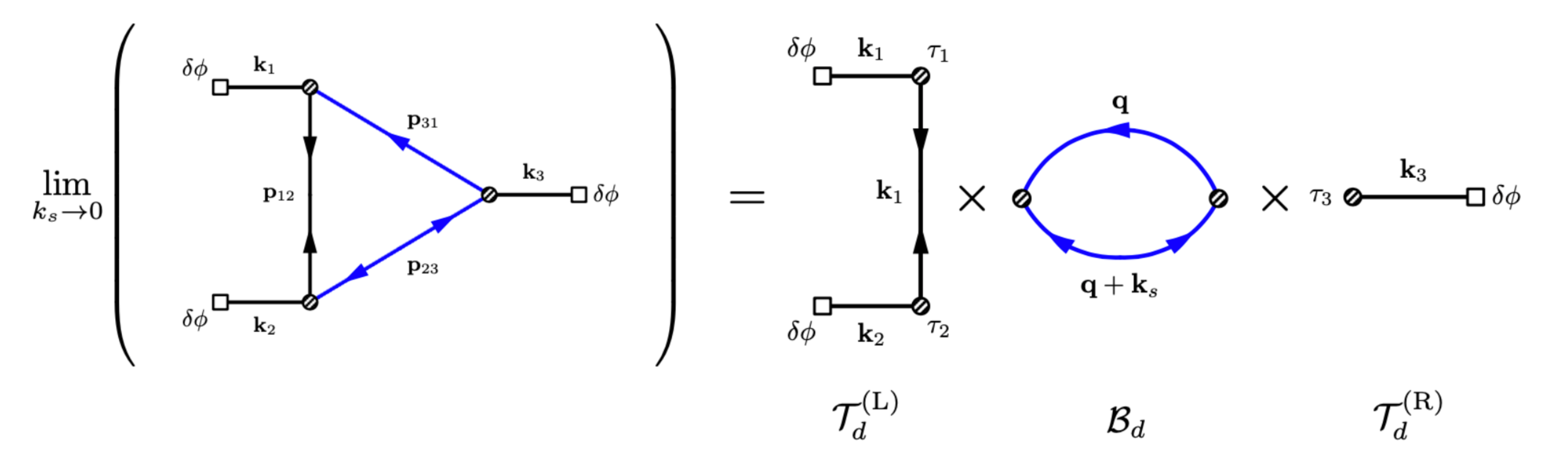

$$\lim_{k_s\to 0}\langle\delta\phi^3\rangle'_{(\mathrm{NLoc})} \simeq \sum_{d=\pm}\sum_{a,b,c=\pm} abc\,\mathcal{T}^{(\mathsf{L})}_{(d),ab}(\mathbf{k}_1,\mathbf{k}_2)\,\mathcal{B}_{(d),abc}(\mathbf{k}_s)\,\mathcal{T}^{(\mathsf{R})}_{(d),c}(\mathbf{k}_3)$$

Left diagram

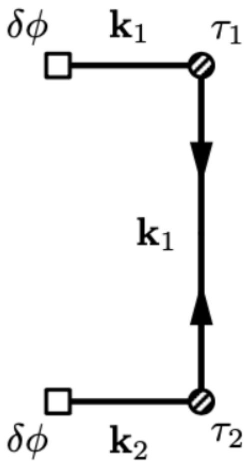

$\mathcal{T}_d^{(\mathrm{L})}$

$$\mathcal{T}^{(\mathsf{L},7)\ \dot{\alpha}}_{(d),ab\quad\ \dot{\beta}}(\mathbf{k}_1) = \left(\frac{-\mathrm{i}}{\Lambda}\right)^2 \int_{-\infty}^{0} \mathrm{d}\tau_1 \mathrm{d}\tau_2\, (-\tau_1)^{\mathrm{i}d\tilde{\nu}} (-\tau_2)^{\mathrm{i}d\tilde{\nu}} \\ \times \mathcal{F}_{\mu a}(\mathbf{k}_1, \tau_1)\, \bar{\sigma}^{\mu\dot{\alpha}\alpha}\, \hat{D}_{ab\alpha}{}^{\beta}(\mathbf{p}_{12}, \tau_1, \tau_2)\, \sigma^{\nu}_{\beta\dot{\beta}}\, \mathcal{F}_{\nu b}(\mathbf{k}_2, \tau_2)$$

Direct evaluation is difficult because the fermion mode functions involve special functions

Earlier work therefore relied on a saddle-point approximation

X. Chen, Y. Wang, and Z.-Z. Xianyu, JHEP 09 (2018) 022
A. Hook, J. Huang, and D. Racco, JHEP 01 (2020) 105

We reduce the calculation to a set of seed integrals and derive analytic expressions.

$$\begin{aligned}\mathcal{I}_{ab}^{p_1p_2} &= k^{1+p_1}k^{1+p_2}\int_{-\infty}^{0}\mathrm{d}\tau_1\mathrm{d}\tau_2\, e^{\mathrm{i}ak\tau_1}e^{\mathrm{i}bk\tau_2}(-\tau_1)^{p_1}(-\tau_2)^{p_2}D_{ab}(\mathbf{k},\tau_1,\tau_2)\\ &= \int_{0}^{\infty}\mathrm{d}z_1\mathrm{d}z_2\, e^{-\mathrm{i}az_1}e^{-\mathrm{i}bz_2}z_1^{p_1}z_2^{p_2}D_{ab}(\mathbf{k},z_1,z_2)\,,\end{aligned}$$

For example, one of the seed integrals is

$$\mathcal{I}^{p_1p_2}_{\oplus\oplus\ \alpha\dot\beta} = \begin{pmatrix} A_1^{p_1p_2}-B_2^{p_1p_2} & 0\\ 0 & A_2^{p_1p_2}-B_1^{p_1p_2}\end{pmatrix}_{\alpha\dot\beta}$$

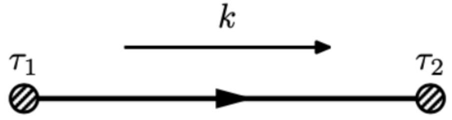

$$\equiv D_{ab_{\alpha\dot\beta}}(\mathbf{k},\tau_1,\tau_2)$$

$$\begin{aligned}A_1^{p_1p_2} &= \int_0^\infty \mathrm{d}z_1\int_0^\infty \mathrm{d}z_2\, e^{-\mathrm{i}z_1}e^{-\mathrm{i}z_2}z_1^{p_1}z_2^{p_2}u_+(z_1)u_+^\dagger(z_2)\theta(z_2-z_1)\\ &= \tilde m^2 e^{\pi\tilde\lambda}I^{p_1p_2}(1+\mathrm{i}\tilde\lambda+\mathrm{i}\tilde\nu,1+\mathrm{i}\tilde\lambda-\mathrm{i}\tilde\nu,\mathrm{i}\tilde\lambda+\mathrm{i}\tilde\nu)\,,\end{aligned}$$

$$\begin{aligned}I^{p_1p_2}(x,y,z) = {}& \mathrm{i}2^{-2-p_1-p_2}e^{-\frac{\mathrm{i}\pi}{2}(p_1+p_2)}\pi\,\mathrm{csch}(2\pi\tilde\nu)\,\Gamma(2+p_1+p_2)\\ &\times\Bigg[\frac{e^{-\pi\tilde\nu}}{\Gamma(x)}\Gamma(1+p_1-\mathrm{i}\tilde\nu)\,\Gamma(2+p_1+p_2-\mathrm{i}2\tilde\nu)\\ &\times {}_4\tilde F_3\left(\begin{matrix}2+p_1+p_2,\ 1+p_1-\mathrm{i}\tilde\nu,\ y,\ 2+p_1+p_2-\mathrm{i}2\tilde\nu\\ 2+p_1-\mathrm{i}\tilde\nu,\ 3+p_1+p_2-z,\ 1-\mathrm{i}2\tilde\nu\end{matrix}\middle|-1\right)-(\tilde\nu\to-\tilde\nu)\Bigg]\end{aligned}$$

Bubble diagram

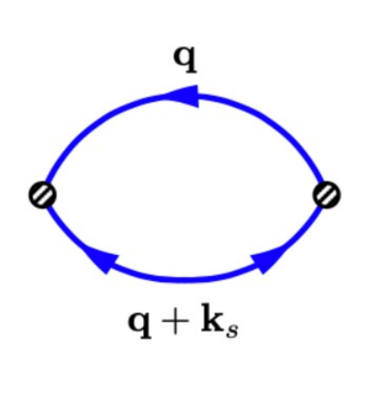

$$\begin{aligned}\mathcal{B}^{(7)}_{(d),abc}{}^{\dot\beta}{}_{\dot\gamma\gamma\dot\alpha} &= \int \frac{\mathrm{d}^3\mathbf{q}}{(2\pi)^3} \frac{\left[\check{D}^{(\mathrm{sym})\,\dot\gamma}{}_{\dot\beta}(\mathbf{p}_{23};\tau_2,\tau_3)\right]_{(\mathrm{NLoc}),d}}{(\tau_2\tau_3)^{\mathrm{i}d\tilde\nu}} \frac{\left[D^{(\mathrm{sym})}_{\gamma\dot\alpha}(\mathbf{p}_{31};\tau_3,\tau_1)\right]_{(\mathrm{NLoc}),d}}{(\tau_3\tau_1)^{\mathrm{i}d\tilde\nu}} \\ &= \delta^{\dot\beta}{}_{\dot\gamma}\sigma_{0\gamma\dot\alpha} \int \frac{\mathrm{d}^3\mathbf{q}}{(2\pi)^3} \frac{\sum_s \left[v_s(\tau_2,\mathbf{p}_{23})u_s^\dagger(\tau_3,\mathbf{p}_{23})\right]_{(\mathrm{NLoc}),d}}{2(\tau_2\tau_3)^{\mathrm{i}d\tilde\nu}} \frac{\sum_s \left[u_s(\tau_3,\mathbf{p}_{31})u_s^\dagger(\tau_1,\mathbf{p}_{31})\right]_{(\mathrm{NLoc}),d}}{2(\tau_3\tau_1)^{\mathrm{i}d\tilde\nu}},\end{aligned}$$

The non-analytic part is from the non-local term of the propagators

$$\left[v_+(\tau_1,\mathbf{k})u_+^\dagger(\tau_2,\mathbf{k})\right]_{(\mathrm{NLoc}),d} = \frac{\tilde{m}e^{\pi\tilde\lambda}\left[\Gamma(-\mathrm{i}2d\tilde\nu)\right]^2}{\Gamma(1-\mathrm{i}\tilde\lambda-\mathrm{i}d\tilde\nu)\Gamma(\mathrm{i}\tilde\lambda-\mathrm{i}d\tilde\nu)}(4k^2\tau_1\tau_2)^{\mathrm{i}d\tilde\nu}$$

$$\left[u_+(\tau_1,\mathbf{k})u_+^\dagger(\tau_2,\mathbf{k})\right]_{(\mathrm{NLoc}),d} = \frac{-e^{\pi\tilde\lambda}\left[\Gamma(-\mathrm{i}2d\tilde\nu)\right]^2}{\Gamma(\mathrm{i}\tilde\lambda-\mathrm{i}d\tilde\nu)\Gamma(-\mathrm{i}\tilde\lambda-\mathrm{i}d\tilde\nu)}(4k^2\tau_1\tau_2)^{\mathrm{i}d\tilde\nu}$$

Non-analytic part
(Cosmological collider signal)

$$\mathcal{B}^{(7)}_{(d),abc}{}^{\dot\beta}{}_{\dot\gamma\gamma\dot\alpha} = \frac{\delta^{\dot\beta}{}_{\dot\gamma}\sigma_{0\gamma\dot\alpha}}{4}\{\Gamma\}_{(d),abc}\int\frac{\mathrm{d}^3\mathbf{q}}{(2\pi)^3}(2\mathbf{q})^{\mathrm{i}2d\tilde\nu}|2(\mathbf{q}+\mathbf{k}_s)|^{\mathrm{i}2d\tilde\nu}$$

$$\mathcal{B}^{(7)}_{(d),abc}{}^{\dot\beta}{}_{\dot\gamma\gamma\dot\alpha} = \frac{\delta^{\dot\beta}{}_{\dot\gamma}\sigma_{0\gamma\dot\alpha}}{4}\{\Gamma\}_{(d),abc}\int\frac{\mathrm{d}^3\mathbf{q}}{(2\pi)^3}(2\mathbf{q})^{\mathrm{i}2d\tilde\nu}|2(\mathbf{q}+\mathbf{k}_s)|^{\mathrm{i}2d\tilde\nu}$$

- The cosmological collider signal is from the integration of the loop momentum
- The integration of the momentum is UV divergent
- However, the non-analytic part is convergent and it is dominated by the soft region q <~ ks
- A naive momentum cut off will include regular dependent term
- It can be extracted using analytic continuation

$$\mathcal{L}_{\text{bubble}}(k_s) = \int\frac{\mathrm{d}^3\mathbf{q}}{(2\pi)^3}|\mathbf{q}|^{-2a}|\mathbf{q}+\mathbf{k}_s|^{-2b} = \frac{k_s^{3-2a-2b}}{(4\pi)^{3/2}}\boxed{\frac{\Gamma\left(a+b-\frac{3}{2}\right)\Gamma\left(\frac{3}{2}-b\right)\Gamma\left(\frac{3}{2}-a\right)}{\Gamma(a)\Gamma(b)\Gamma(3-a-b)}}$$

This factor is around 10^{-4} , which is missed in previous work using dimensional analysis

Main Result: Analytic Expression

$$f_{\rm NL}^{\rm CC} \approx \left| \frac{5H_{\rm inf}^3}{18(2\pi^2 P_\zeta)^2 \dot{\phi}_0^3 \Lambda^3} S_3^{1-{\rm i}\tilde{\nu},\,1-{\rm i}\tilde{\nu}} \frac{2^{-2-4{\rm i}\tilde{\nu}} e^{2\pi\tilde{\lambda}-5\pi\tilde{\nu}} \tilde{m}^3 \pi ({\rm i}+2\tilde{\nu})^2 (3{\rm i}+4\tilde{\nu}) \Gamma(2{\rm i}\tilde{\nu})}{\Gamma(1-{\rm i}\tilde{\lambda}+{\rm i}\tilde{\nu})^2 \Gamma(5-4{\rm i}\tilde{\nu}) \Gamma({\rm i}\tilde{\lambda}+{\rm i}\tilde{\nu}) \Gamma(1+{\rm i}\tilde{\lambda}+{\rm i}\tilde{\nu})} \right|$$

$$\begin{aligned} S_3^{1-{\rm i}\tilde{\nu},\,1-{\rm i}\tilde{\nu}} &= 2^{-3+2{\rm i}\tilde{\nu}} e^{\pi\tilde{\lambda}-2\pi\tilde{\nu}} \tilde{m}\pi\Gamma(2-2{\rm i}\tilde{\nu}) \\ &\times \Bigg\{ -\frac{1}{(-{\rm i}+\tilde{\lambda}-\tilde{\nu})(2{\rm i}-\tilde{\lambda}+\tilde{\nu})^2 \Gamma(2+{\rm i}\tilde{\lambda}-{\rm i}\tilde{\nu})\Gamma(-1+2{\rm i}\tilde{\nu})\Gamma(-{\rm i}\tilde{\lambda}-{\rm i}\tilde{\nu})} \\ &\quad + \frac{1}{(-{\rm i}+\tilde{\lambda}-\tilde{\nu})(-2{\rm i}+\tilde{\lambda}-\tilde{\nu})\Gamma(-{\rm i}\tilde{\lambda}-{\rm i}\tilde{\nu})} \Bigg[{\rm i}\, {}_3\tilde{F}_2\left(\begin{matrix} 2,\ -2-{\rm i}\tilde{\lambda}+{\rm i}\tilde{\nu},\ 2-2{\rm i}\tilde{\nu} \\ 3+{\rm i}\tilde{\lambda}-{\rm i}\tilde{\nu},\ -1+2{\rm i}\tilde{\nu} \end{matrix} ; -1 \right) \\ &\quad + 4(-2{\rm i}+\tilde{\lambda}-\tilde{\nu})(1-{\rm i}\tilde{\nu})\, {}_3\tilde{F}_2\left(\begin{matrix} 3,\ -1-{\rm i}\tilde{\lambda}+{\rm i}\tilde{\nu},\ 3-2{\rm i}\tilde{\nu} \\ 4+{\rm i}\tilde{\lambda}-{\rm i}\tilde{\nu},\ 2{\rm i}\tilde{\nu} \end{matrix} ; -1 \right) \Bigg] \\ &\quad - {\rm i} e^{2\pi\tilde{\nu}} \frac{\Gamma(4-2{\rm i}\tilde{\nu})\Gamma(4-4{\rm i}\tilde{\nu})}{\Gamma(-{\rm i}\tilde{\lambda}+{\rm i}\tilde{\nu})}\, {}_4\tilde{F}_3\left(\begin{matrix} -{\rm i}\tilde{\lambda}-{\rm i}\tilde{\nu},\ 2-2{\rm i}\tilde{\nu},\ 4-2{\rm i}\tilde{\nu},\ 4-4{\rm i}\tilde{\nu} \\ 1-2{\rm i}\tilde{\nu},\ 3-2{\rm i}\tilde{\nu},\ 5+{\rm i}\tilde{\lambda}-3{\rm i}\tilde{\nu} \end{matrix} ; -1 \right) \Bigg\}. \end{aligned}$$

Large lambda limit

$$f_{\rm NL}^{\rm CC} \simeq \frac{5\pi^{\frac{5}{2}}}{2^8 9\sqrt{2}} P_\zeta \tilde{M}_R^4 \tilde{\lambda}^{\frac{9}{2}} e^{-\frac{9\pi}{2}(\tilde{\nu}-\tilde{\lambda})}$$

$$e^{-\frac{9\pi}{2}(\tilde{\nu}-\tilde{\lambda})} \sim e^{-\frac{9\pi}{4}(\tilde{M}_R^2/\tilde{\lambda})}$$

The summed fermion-loop contribution has no additional angular dependence and effectively mimics a scalar-exchange clock signal

Comparison with previous result

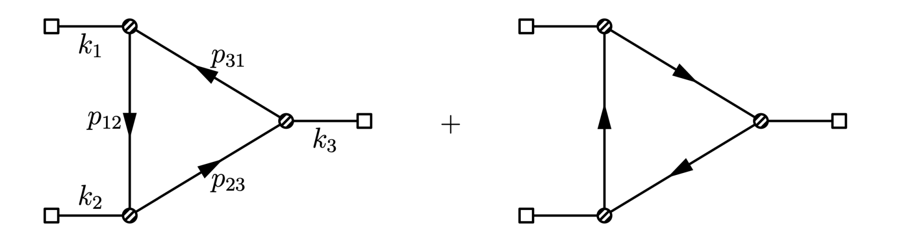

X. Chen, Y. Wang, and Z.-Z. Xianyu, JHEP 09 (2018) 022
A. Hook, J. Huang, and D. Racco, JHEP 01 (2020) 105

$$\Lambda = (5, 4, 3, 2)\dot{\phi}_0^{1/2}$$

- The left subdiagram TL was estimated with a saddle-point approximation
- The bubble subdiagram was evaluated at a characteristic loop momentum ks, rather than through the full integration
- Under these assumptions, the loop signal appeared potentially observable

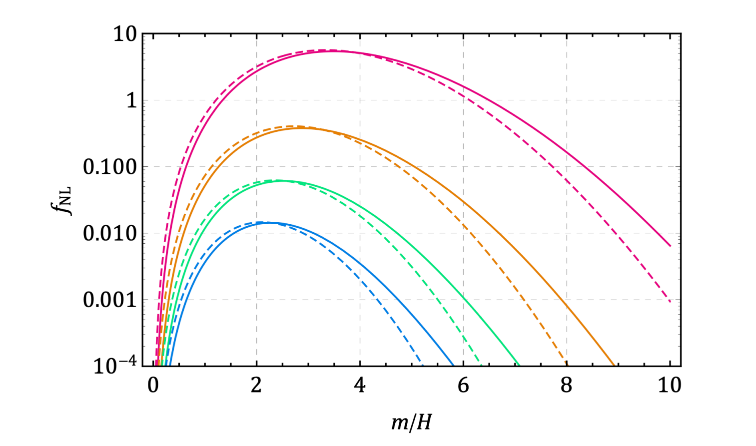

We find that the previously considered benchmark contribution is much smaller

What changes numerically?

- The saddle-point approximation can differ substantially from the exact result in some mass ranges.
- The full loop integration brings an additional suppression factor of order 10^{-4}.
- Taken together, the earlier estimate can be too large by roughly six orders of magnitude.

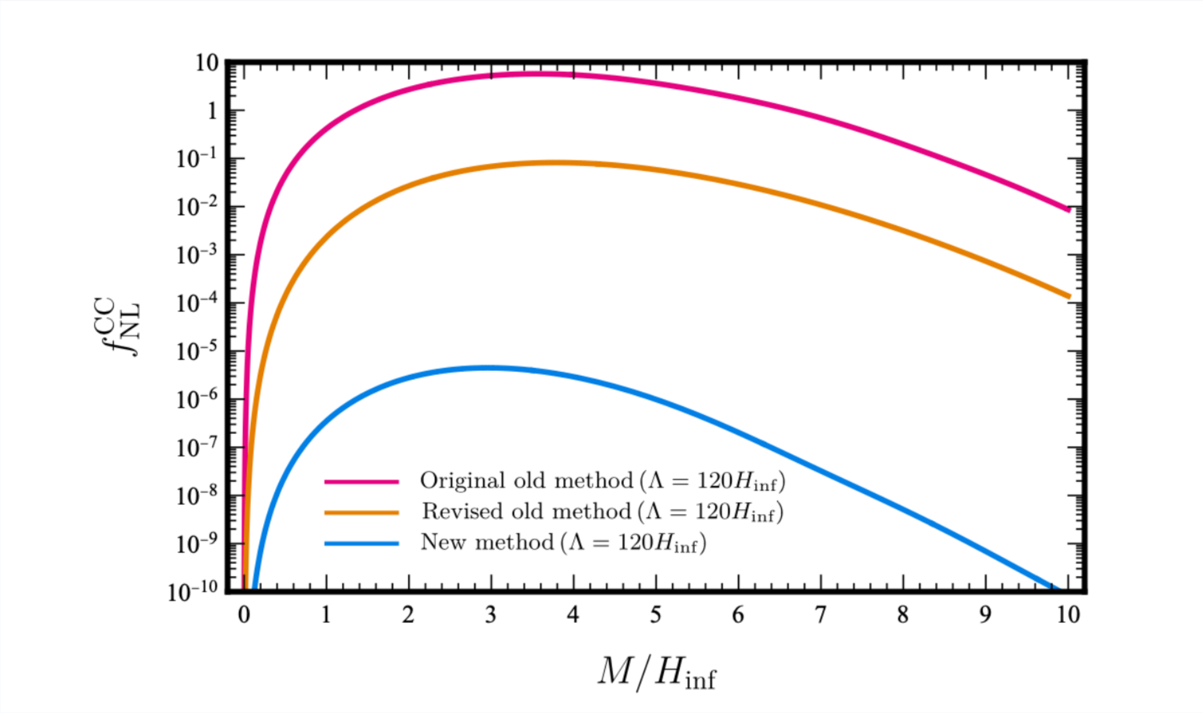

If one corrects only the old benchmark contribution, the seesaw signal appears hopelessly small.

But that is not the full answer: many diagrams were missing

The earlier literature included only a subset of the allowed RH-neutrino loop diagrams

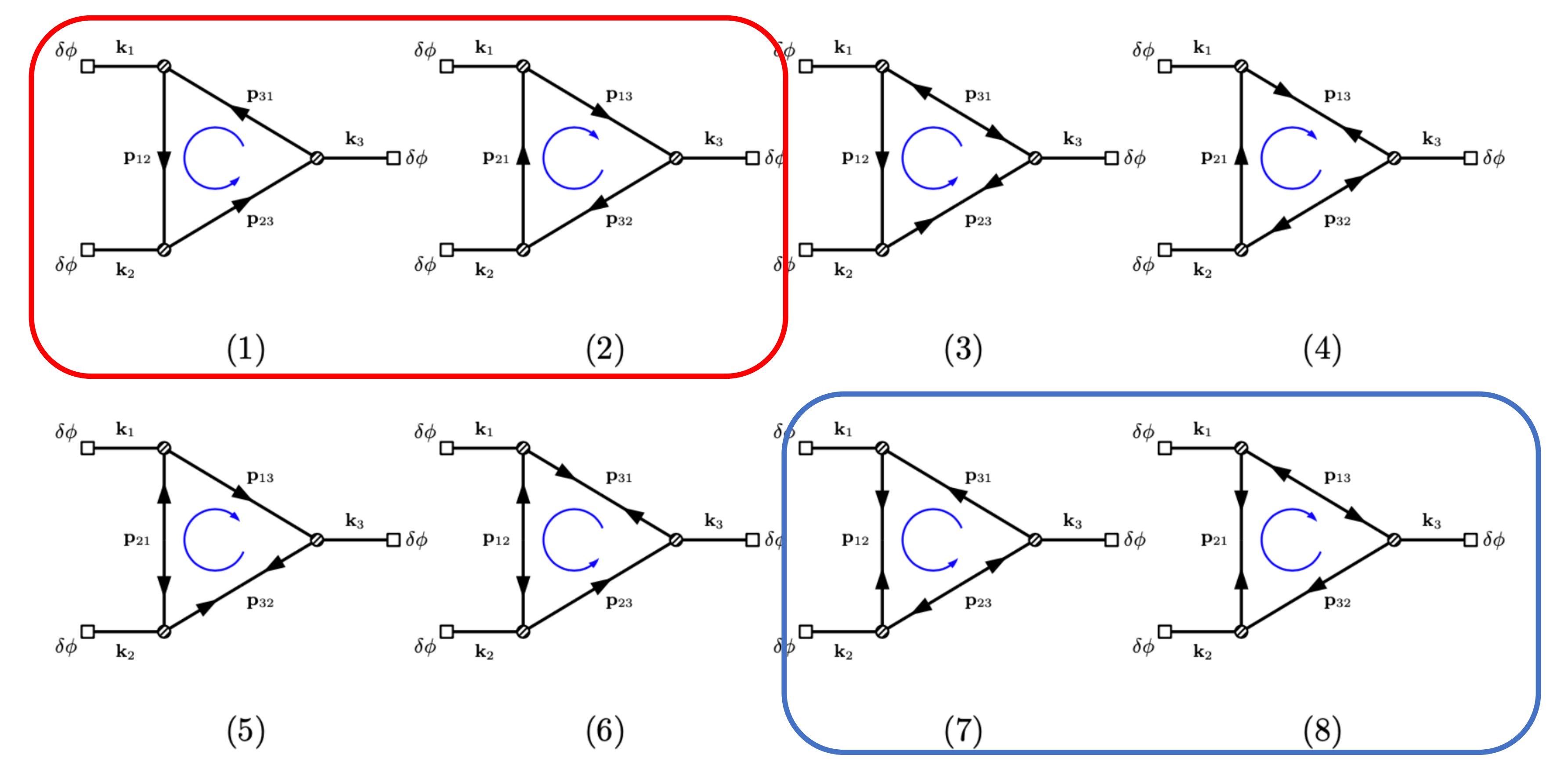

Full Result: An Observable Window Reappears after Summing All Diagrams

$$\lambda \sim \dot{\phi}/\Lambda \quad \lambda = (60,\, 45,\, 36,\, 30)\, H_{\rm inf}$$

- New diagrams can dominate over the older benchmark piece.
- In part of parameter space, the total RH-neutrino loop signal reaches an observable level.

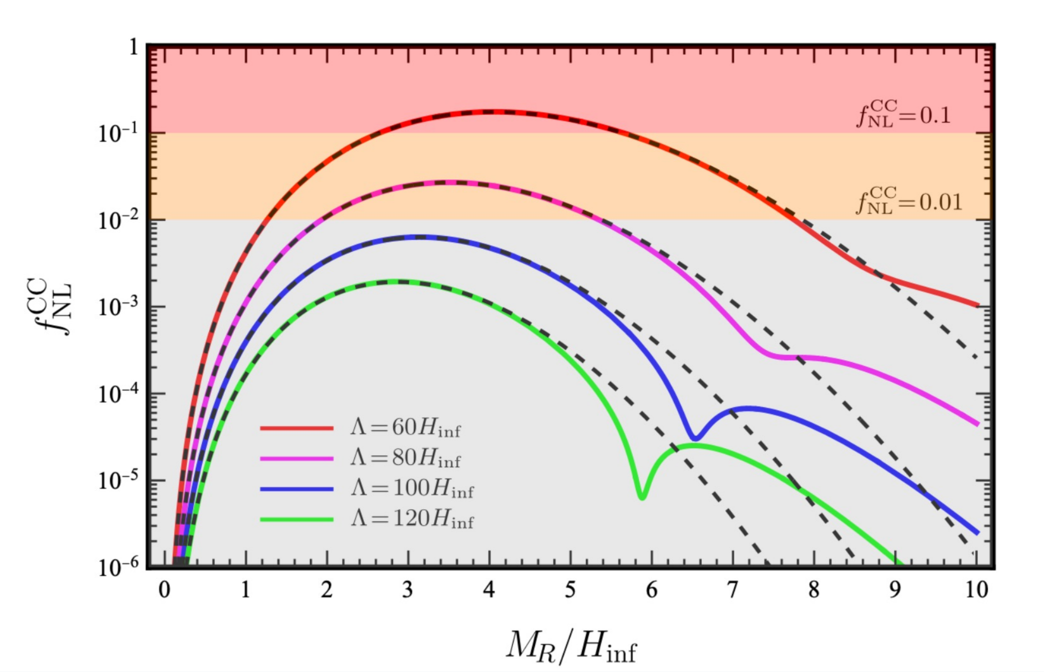

$$e^{-\pi m/H} \to e^{-\pi m^2/\lambda H}$$

Summary

- Right-handed neutrinos are motivated by neutrino masses and leptogenesis, but their natural scale is extremely high
- In the relevant cosmological-collider setup, fermionic signals arise only from loops, so quantitative control matters
- RH-neutrino loops can still generate an observable nonlocal bispectrum in part of parameter space

Analytic result versus saddle point approximation